# NEAR-FIELD SCANNING MICROWAVE MICROSCOPY: MEASURING LOCAL MICROWAVE PROPERTIES AND ELECTRIC FIELD DISTRIBUTIONS

B. J. Feenstra, C. P. Vlahacos, Ashfaq S. Thanawalla, D. E. Steinhauer, S. K. Dutta, F. C. Wellstood and
Steven M. Anlage

*Center for Superconductivity Research, Department of Physics,*
*University of Maryland, College Park, MD 20742-4111, USA*

## Abstract

We describe the near-field scanning microwave microscopy of microwave devices on a length scale much smaller than the wavelength used for imaging. Our microscope can be operated in two possible configurations, allowing a quantitative study of either material properties or local electric fields.

## Introduction

In recent years, several novel methods of scanning probe microscopy have been developed. Generally speaking one can divide these methods into two main approaches, driven by distinct motivations. In the first approach the main goal is to study material properties, preferably on the smallest possible length scale. Examples of such techniques are atomic force microscopy (AFM) and scanning tunneling microscopy (STM) [1, 2], which have achieved atomic scale spatial resolution. The second objective is the investigation of fields, both electric and magnetic, emitted by operating devices. An example of such a technique is scanning microwave microscopy[3, 4]. For devices operating in the microwave range, a scanning technique at microwave frequencies will be useful for diagnosing circuit problems. Despite the relatively long wavelength, of the order of mm's to cm's, spatial resolution below 1 $\mu$m can be achieved by operating in the so-called near-field limit[5, 6]. In this paper we will illustrate the versatility of near-field scanning microwave microscopy, by showing results on local material properties as well as on electromagnetic field imaging in close proximity to operating devices.

## Experimental Setup

Fig. 1 shows a schematic of our experimental setup. The microwave microscope can be operated in two distinct configurations: what we call the reflecting mode (solid lines in Fig. 1) and the receiving mode (dashed-dotted lines).
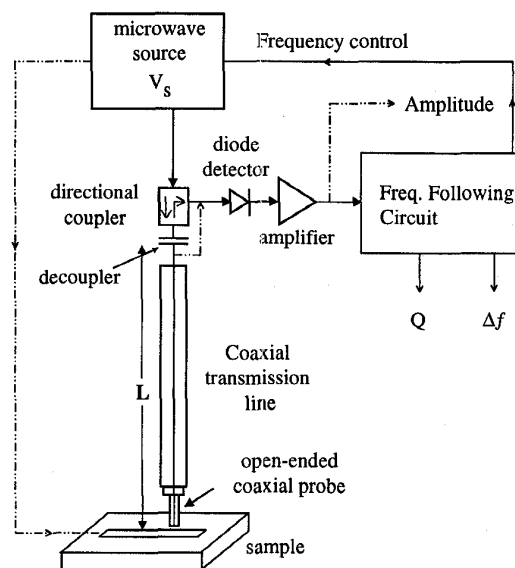


Figure 1: *Experimental setup, showing the reflecting mode (solid lines) and the receiving mode (dash-dotted lines).*

## Reflecting Mode

In the reflecting mode, a microwave signal is fed through a coaxial transmission line which has been capacitively coupled to the source and ends in a rigid open-ended coaxial probe. This creates a resonant circuit, in which the resonant frequency $f_0$ and the quality factor $Q$ are modified by the sample which is in close proximity to the open end of the probe. Using a lock-in based frequency-following circuit[7] we measure the shift of the resonance $\Delta f$ as the sample is scanned under the probe. We can also measure the strength of the signal at twice the lock-in modulation frequency. The latter is related to the curvature of the resonance peak and is a measure of the $Q$ of the system[8]. By measuring

both quantities simultaneously we obtain information about the real and the imaginary part of the complex dielectric function, $\epsilon$, of the sample.

### Receiving Mode

A slightly modified configuration (dash-dotted lines in Fig. 1) can be used to measure electric fields emitted by operating microwave devices. In this case, microwave power is fed directly to the device and the coaxial probe senses the electric fields from the sample. The microwave power measured by the probe is fed to the diode detector directly, bypassing the decoupler, directional coupler and the resonant transmission line. The measured amplitude can be converted to electric field, using additional information about the setup[4].

## Material Properties

The data analysis can be complicated considerably when, in addition to the variations in material properties, the sample exhibits topographic features[9]. Several methods have been used to separate out the topography. The simplest approach is to scan the same region twice, initially recording the topography[10]. Another solution is to measure the probe-sample separation independently, and use this information in a feedback loop to maintain the probe at a constant height[11].

Our system is especially sensitive to topographic features when we measure the frequency shift $\Delta f$. Figure 2 shows a glass chip in which various topographic features were etched. By measuring the height dependence of the frequency shift at one particular spot on the sample (Fig. 3), we calibrate the relation between $\Delta f$ and the height $h$. Next, we fit the response to an empirical function, shown as the solid line. We can then use this function to determine the absolute height of the probe above the entire sample[12].

Figure 4a shows such a topographic image taken using a probe with an inner conductor diameter of 100 $\mu m$ at 50 $\mu m$ above the highest point on the sample. We are able to discern height changes as small as 55 nm, this figure being limited by the frequency stability of the microwave source. A line cut, taken along the dashed line in Figure 2, reveals more details (see Fig. 4b). The dashed line shows the width of the slits, all of which are 30 $\mu m$ deep. A fair agreement is obtained for most of the line-cut, although it can be seen that for features comparable to or smaller than the probe size, the height measured with the microwave microscope suffers from averaging effects, yielding results which are too shallow. The effective spatial resolution is $d \sim 100 \mu m \approx \lambda/300$.
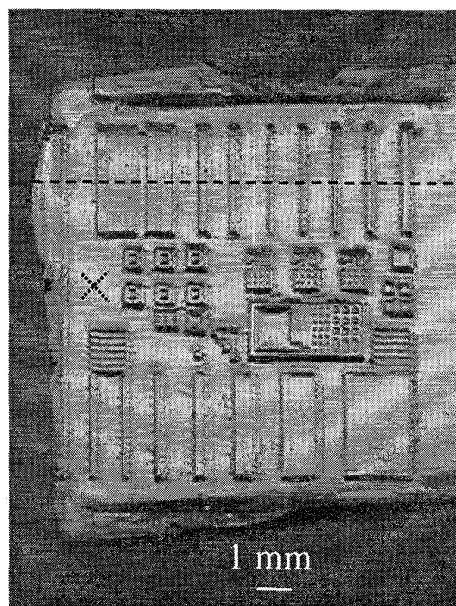


Figure 2: *Photograph of a glass chip which has a variety of structures etched into the surface. The cross indicates the position at which the calibration curve in Fig. 3 was measured.*
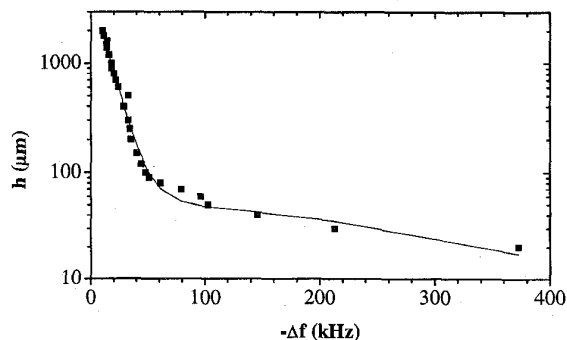


Figure 3: *Calibration curve correlating frequency shift $\Delta f$ and height $h$, measured at 9.6 GHz using a 100 $\mu m$ probe.*

## Electric Field Imaging

An important potential application of microwave microscopy is for the diagnosis of problems in integrated circuits. Since many circuits operate at microwave frequencies, it is essential to have a technique that searches
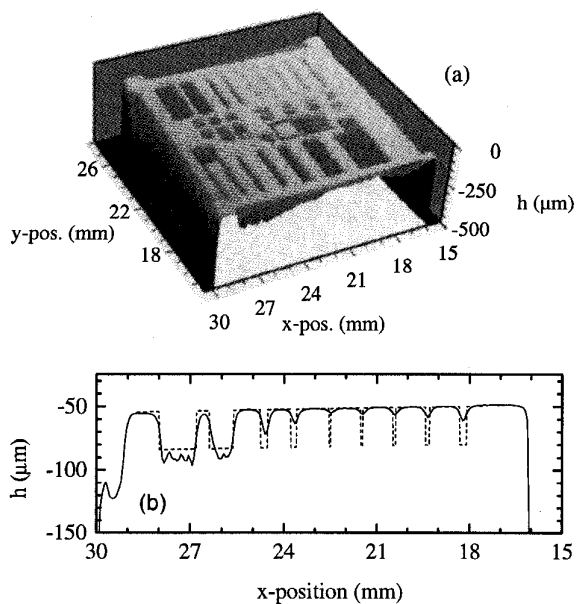
Figure 5: *Photograph of Cu-microstrip resonator. Also indicated are the position at which the power is capacitively coupled into the resonator ($P_{in}$) and the position at which the frequency response was measured (A). The chip is enclosed in a Cu-package.*

Figure 4: *(a): Topographic image of the glass chip, as measured with the microwave microscope at 9.6 GHz. (b): Line cut, taken along the dashed line in Fig. 2, showing the depth profile in more detail.*

for faults at the operating frequency. In addition, a non-destructive technique is desired. Near-field microwave microscopy offers the possibility of scanning the coaxial probe in close proximity to an operating device, thereby sensing the electric field component normal to the face of the probe[4].

Much of our research is devoted to the study of superconducting devices. For this reason, we have developed a microscope which works at temperatures down to 4.2 K[13]. In Fig. 5 we show a Cu-microstrip resonator. The groundplane of the microstrip is also made of copper, and the microstrip dimensions are $8 \times 1$ mm. Fixing a 200 $\mu m$ diameter probe at 1 mm above position A, and coupling the microwave power in at $P_{in}$, we measured the signal picked up by the probe as a function of frequency. The response at 300 K and 77 K is shown in Fig. 6. Upon lowering the temperature, both the signal picked up by the probe and the $Q$ of the resonator are enhanced considerably.

From Fig. 6, we also see that the resonant frequency of the microstrip increases at low temperatures. One possible cause is that the decreased inductance (reduced skin depth) at lower temperatures will shift the resonant
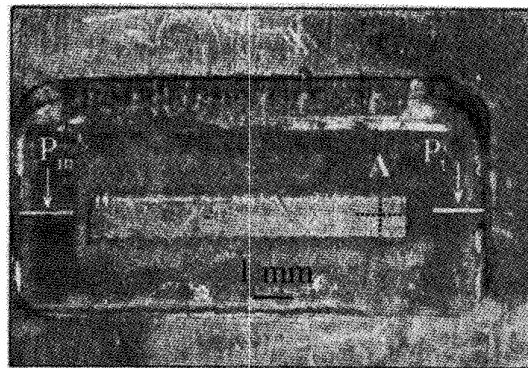
frequency upward. This is consistent with the reduced losses at 77 K, clearly visible in the enhanced quality factor of the resonance. Assuming that the enhanced $Q$ can be associated entirely with the Cu-microstrip, we can calculate how large the corresponding frequency shift will be. For $Q(77)/Q(300) = 4$ one expects a change in frequency of approximately 0.1 %, giving $\Delta f \approx 10$ MHz. Since the measured frequency shift is much larger ($\approx 300$ MHz), it is clear that this effect plays only a minor role. Secondly, thermal contraction will also increase the resonant frequency. Assuming a thermal contraction coefficient $\alpha = \Delta L/L = 10^{-5}/K$, the relative change of the length of the resonator would be approximately $2 \times 10^{-3}$, implying a similar change in the resonant frequency. Finally, the presence of the probe close to the resonator imposes a perturbation on the latter. Since this is an electric field perturbation, the resonant frequency will tend to shift down. Part of the shift may hence be due to the fact that the coupling between the probe and the Cu-resonator is less at low temperatures.

To image the sample, we fixed the frequency at the resonance peak and scanned the sample underneath the coaxial probe, measuring the electric field as a function of position. The resulting xy-scan at 77 K can be seen in Fig. 7; the probe was kept at a constant distance of 350 $\mu m$ above the sample. We see that the electric field peaks at the ends of the stripline and vanishes in the middle, as expected for the fundamental voltage mode. Close to the power pin (near x = 7 mm) the perturbing effect of the probe is more serious than in the rest of the image, causing the amplitude to decrease slightly.
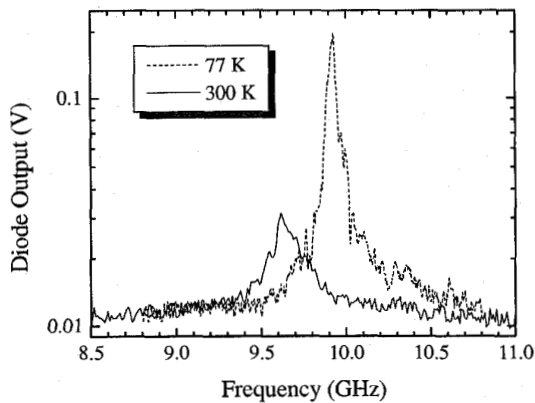
967

Figure 6: *Frequency response of the Cu-microstrip, at 300 K (solid line) and 77 K (dashed line).*
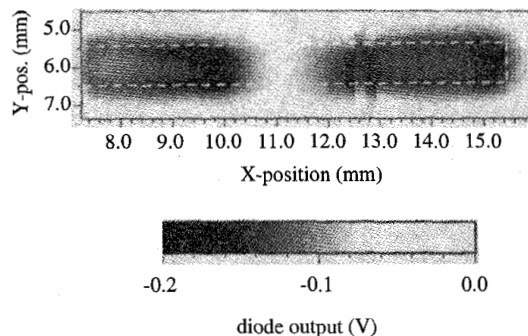


Figure 7: *Electric field pattern above a 77 K Cu-microstrip line, operating at its fundamental resonant frequency, 9.90 GHz. The edges of the stripline are indicated by the dashed lines.*

## Conclusions

We have demonstrated the ability of near-field scanning microscopy to provide quantitative information on material properties and electric field distributions at microwave frequencies. We are able to study microwave properties at a length scale as small as $\lambda/300$, operating at temperatures varying from 4.2 to 300 K.

## References

[1] L. J. Balk and M. Maywald, 'Scanning Force Microscopy of Semiconductor Materials and Devices', Mat. Sci. Eng. B **24**, 203 (1994).

[2] Ivan Amato, 'Candid Camera for the Nanoworld', Science **276**, 579 (1997).

[3] Thomas P. Budka, Scott D. Waclawik, and Gabriel M. Rebeiz, 'A Coaxial 0.5-18 GHz Near Electric Field Measurement System for Planar Microwave Circuits Using Integrated Probes', IEEE Trans. Microwave Theor. Tech. **44**, 2174 (1996).

[4] S. K. Dutta *et al.*, 'Quantitative Electric Field Imaging using a Near-Field Scanning Microwave Microscope', in preparation.

[5] C. A. Bryant and J. B. Gunn, 'Noncontact Technique for the Local Measurement of Semiconductor Resistivity', Rev. Sci. Instr. **36**, 1614 (1965).

[6] E. A. Ash and G. Nicholls, 'Super-Resolution Aperture Scanning Microscope', Nature **237**, 510 (1972).

[7] D. E. Steinhauer *et al.*, 'Surface Resistance Imaging with a Scanning Near-Field Microwave Microscope', Appl. Phys. Lett. **71**, 1736 (1997).

[8] D. E. Steinhauer *et al.*, 'Quantitative Imaging of Sheet Resistance with a Scanning Near-Field Microwave Microscope', Appl. Phys. Lett. **72**, 861 (1998).

[9] B. Knoll *et al.*, 'Contrast of Microwave Near-Field Microscopy', Appl. Phys. Lett. **70**, 2667 (1997).

[10] Y. E. Strausser and M. G. Heaton, 'Scanning Probe Microscopy: Technology and Inovations', American Laboratories **26**, 20 (1994).

[11] J. W. P. Hsu, Mark Lee, and B. S. Deaver, 'A Nonoptical Tip-Sample Distance Control Method for Near-Field Scanning Optical Microscopy using Impedance Changes in an Electromechanical System', Rev. Sci. Instr. **66**, 3177 (1995).

[12] C. P. Vlahacos *et al.*, 'Quantitative Topographic Imaging using a Near-Field Scanning Microwave Microscope', Appl. Phys. Lett. **72**, XXX (1998).

[13] Ashfaq S. Thanawalla *et al.*, 'Microwave Near-Field Imaging of Electric Fields in a Resonant Superconducting Microwave Device', in preparation.